Theoretical Study on the Mechanism of Formation of Cyanate Resins

Satoshi Okumoto

Matsushita Electric Works, Ltd., 1048, Kadoma, Osaka 571-8686, Japan

Shinichi Yamabe*

Department of Chemistry, Nara University of Education, Takabatake-cho, Nara 630-8528, Japan

Received January 5, 1999

Ab initio calculations of a formation reaction of a triazine ring were performed. From the model substrate, methyl cyanate, a concerted association path with C_{3h} symmetry was first examined. In terms of energy changes, this path was found to be unlikely. Second, a stepwise path assisted by a water cluster was tested. But, this path was found to be of a relatively high amount of activation energy in the first additional step. Third, a zinc formate was used as a catalyst, and the reaction was computed to have a reasonable stepwise route for formation of the six-membered triazine ring. Fourth, the reaction promoted by a hydronium ion was shown to generate a ring-closure mechanism similar to that caused by the zinc catalyst. Thus, the crucial role of catalysts coordinated to the σ lone-pair orbital of the cyanate nitrogen atom was verified.

Introduction

With current trends toward increased circuit densities, shorter propagation delays, elevated operating temperatures, and higher reliability, new advanced materials for use in conventional electronic circuit boards are being developed to satisfy these demands. Among those materials, cyanate resin is considered to be very promising. The cyanate resin 2 most commonly in use is based on bisphenol A dicyanate (BPACN) **1** derived from bisphenol A.[1−4] The curing reaction is shown in Scheme 1. Cyanate resins have many excellent properties, such as good thermal stability, high transition temperature, and low dielectric constants over wide ranges of frequency and temperature.

Those resins are produced by the curing reaction which has been investigated extensively through NMR, FT-IR, and kinetic measurements.[5,6] Yet despite these careful product analyses and kinetic studies, the reaction mechanism of triazine ring formation remains unelucidated. An approach to this issue lies in the catalyst. A typical catalyst in Scheme 1 is a small amount (∼200 ppm) of zinc octanoate $Zn(C_7H_{15}COO)_2$. When *p*-*tert*-butylphenyl cyanate, *p*-$(CH_3)_3C$-C_6H_4-$OC^{15}N$, was heated (100 °C, 5 h in methyl ethyl ketone and acetone-d_6), no reactions were observed through the ^{15}N solution NMR spectra. On the other hand, when the substrate was heated (100 °C, 1 h) with zinc octanoate as a catalyst, formation of the triazine ring was observed.[5] The reaction of Scheme 1 is accelerated also by water.[5,6] In contrast to extensive experimental studies, the curing reactions of cyanate polymer resins have not been examined theoretically. To elucidate the reaction mechanism of Scheme 1 and the role of catalysts, ab initio calculations were carried out on a model compound, methyl cyanate (Me-OCN) with H_2O, $Zn(HCOO)_2$, and H_3O^+ catalysts, as shown in Scheme 2. The present analyses are expected to be useful in seeking new catalysts for the efficient syntheses of cyanate resins.

Methods of Computations

Ab initio calculations were performed using the GAUSSIAN 94[7] program package on a CONVEX SPP 1200/XA computer at the Information Processing Center of Nara University of Education, and on a SGI Indigo2 computer at Matsushita Electric Works, Ltd. RHF/3-21G(*) and RHF/6-311G* methods were applied to geometry optimizations and subsequent vibrational analyses. Geometries were fully optimized with the threshold convergence criteria (0.000450) of GAUSSIAN94. First, transition states (TSs) were determined by RHF/3-21G*. Second, RHF/3-21G* IRC (Intrinsic Reaction coordinate) calculations[8] were performed to locate intermediates. Third, RHF/6-311G* geometries were determined on the basis of the RHF/3-21G* ones. Energies were refined by single-point calculations of the density functional theory of B3-LYP[9] on the 6-311+G-(2d,p) basis set, which is known to be a highly accurate and practical method.[10]

(1) Shimp, D. A.; Christenson, J. R.; Ising, J. *Proceedings of the 34th International Symposium*; SAMPE: Azusa, CA, 1989, p 222.

(2) Wang, D. W. In *Mater. Res. Soc. Symp. Proc.*, **1987**, *108*, 125.

(3) Bogan, G. W.; Lassy, M. E.; Monnerat, G. A.; Woo, E. P. *SAMPE J.* **1988**, *24*, 19.

(4) Wang, D. W. Electronic Packaging Materials Science III. In *Materials Research Society Symposium Proceedings*; Jaccodine, R., Jackson, K. A., Sundahl, R. C., Eds.; Elsevier: New York, 1988; Vol. 108, p 125.

(5) Fyfe, C. A.; Niu, J.; Rettig, S. J.; Burlinson, N. E.; Reidsma, C. M., Wang, D. W.; Poliks, M. *Macromolecules* **1992**, *25*, 6289.

(6) Grenier-Loustalot, M. F., Lartigau, C.; Grenier, P. *Eur. Polym. J.* **1995**, *31*, 1139.

(7) Frisch, M. J.; Trucks, G. W.; Schlegel, H. B.; Gill, P. M. W.; Johnson, B. G.; Robb, M. A.; Cheeseman, J. R.; Keith, T. A.; Petersson, G. A.; Montogomery, J. A.; Raghavachari, K.; Al-Laham, M. A.; Zakrzewski, V. G.; Ortiz, J. V.; Foresman, J. B.; Cioslowski, J.; Stefanov, B. B.; Nanayakkara, A.; Challacombe, M.; Peng, C. Y.; Ayala, P. Y.; Chen, W.; Wong, M. W.; Andres, J. L.; Replogle, E. S.; Gomperts, R.; Martin, R. L.; Fox, D. J.; Binkley, J. S.; Defrees, D. J.; Baker, J.; Stewart, J. P.; Head-Gordon, M.; Gonzalez, C.; Pople, J. A, Gaussian 94 (Revision A.1), Gaussian, Inc., Pittsburgh, PA, 1995.

(8) (a) Fukui, K. *Acc. Chem. Res.* **1981**, *14*, 363. (b) Gonzalez, C.; Schlegel, H. B. *J. Phys. Chem.* **1989**, *90*, 2154. (c) Gonzalez, C.; Schlegel, H. B. *J. Phys. Chem.* **1990**, *94*, 5523.

(9) (a) Becke, A. D. *J. Chem. Phys.* **1993**, *98*, 5648. (b) Becke, A. D. *Phys. Rev.* **1988**, *A38*, 3098. (c) Lee, C.; Yang, W.; Parr, R. G. *Phys. Rev.* **1988**, *B37*, 785. (d) Vosco, S. H.; Wilk, L.; Nusair, M. *Can. J. Phys.* **1980**, *58*, 1200.

(10) Foresman, J. B.; Frisch, A. *Exploring Chemistry with Electronic Structure Methods*; 2nd ed.; Gaussian Inc.: Pittsburgh, PA, 1995; Chapter 7, p 158.

10.1021/jo9900275 CCC: $18.00
Published on Web 05/29/1999

Scheme 1. The Curing Reaction for the BPACN Cyanate Resin

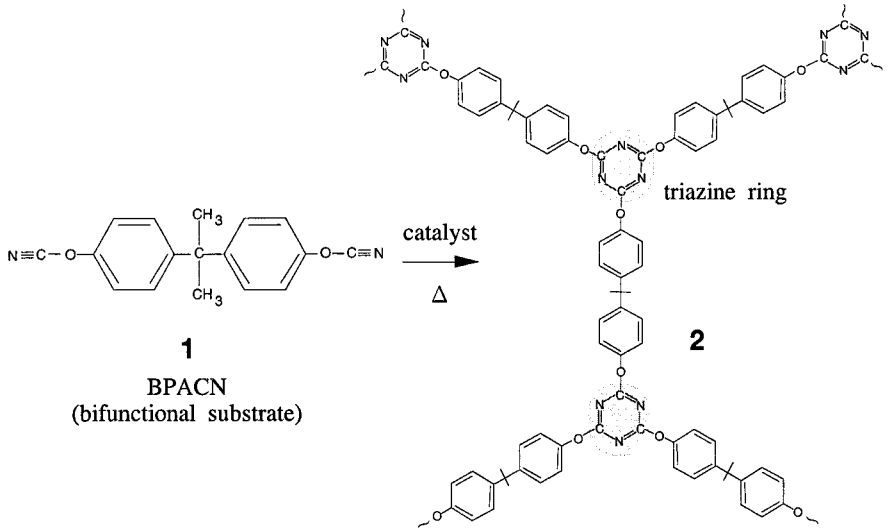

Table 1. Total Energies (in hartrees) and Their Differences (in kcal/mol, parentheses) Relative to Those of Three Separeated Substrates, Methyl Cyanate in Reaction 1. The Corresponding Geometries Are Shown in Figure 1

method	before reaction	intermediate **1**	TS	after reaction
RHF/3-21G	−606.786923 (0)	−616.817517 (−19.1)	−616.725274 (38.7)	−616.925000 (−86.7)
free energy	−616.704318 (0)	−616.701997 (1.5)	−616.600718 (65.0)	−616.786570 (−51.6)
B3-LYP/6-311+G(2d,p)//RHF/3-21G	−624.030069 (0)	−624.046963 (−10.6)	−623.978290 (32.5)	−624.182109 (−95.4)
RHF/6-311G*	−620.404218 (0)	−620.423213 (−11.9)	−620.299491 (65.7)	−620.544580 (−88.1)
B3-LYP/6-311+G(2d,p)//RHF/6-311G*	−624.027510 (0)	−624.045333 (−11.2)	−623.976474 (32.0)	−624.181208 (−96.5)

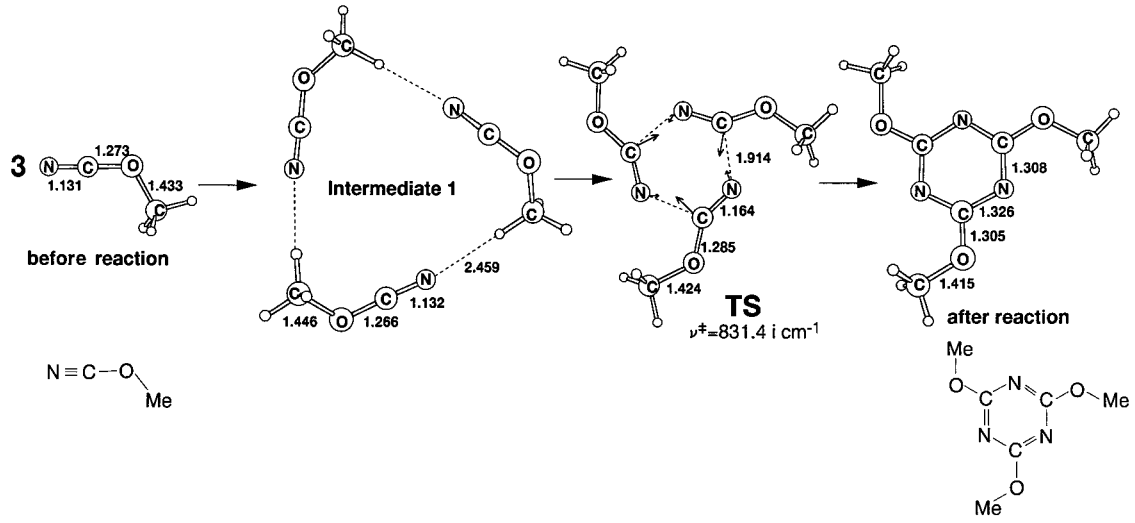

Figure 1. Geometries of the triazine ring formation reaction optimized by the RHF/6-311G* method. TS is a transition state, where the reaction-coordinate vector is sketched. The vector corresponds to the sole imaginary frequency, 831.4 i cm^{-1}. Distances are in angstroms. Empty small circles stand for hydrogen atoms.

Scheme 2. A Model Reaction Treated Here

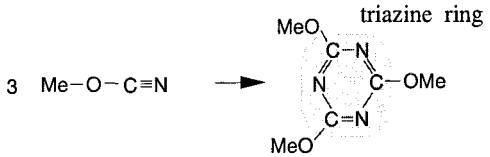

Results of Calculations and Discussions

Reactions of the triazine-ring formation were investigated in the following four ways: (1) reaction without catalytic molecules (gas phase) (reaction 1); (2) reaction with water molecules (reaction 2); (3) reaction with zinc formate, $Zn(HCOO)_2$ (reaction 3); (4) reaction with a hydronium ion (reaction 4). Those four reactions will be compared.

(1) Reaction without Catalytic Molecules. The catalyst-free reaction (reaction 1) was examined in terms of whether the reaction can take place in a concerted or a stepwise manner. In the stepwise route, two substrates (methyl cyanate) are linked first, followed by addition of the third one to the dimer. As a result of geometry optimizations, no stepwise routes were found. Only the concerted ring-formation reaction was obtained (Figure 1), which was verified by the reaction-coordinate vector at the TS. The reaction system has a C_{3h} symmetry, and

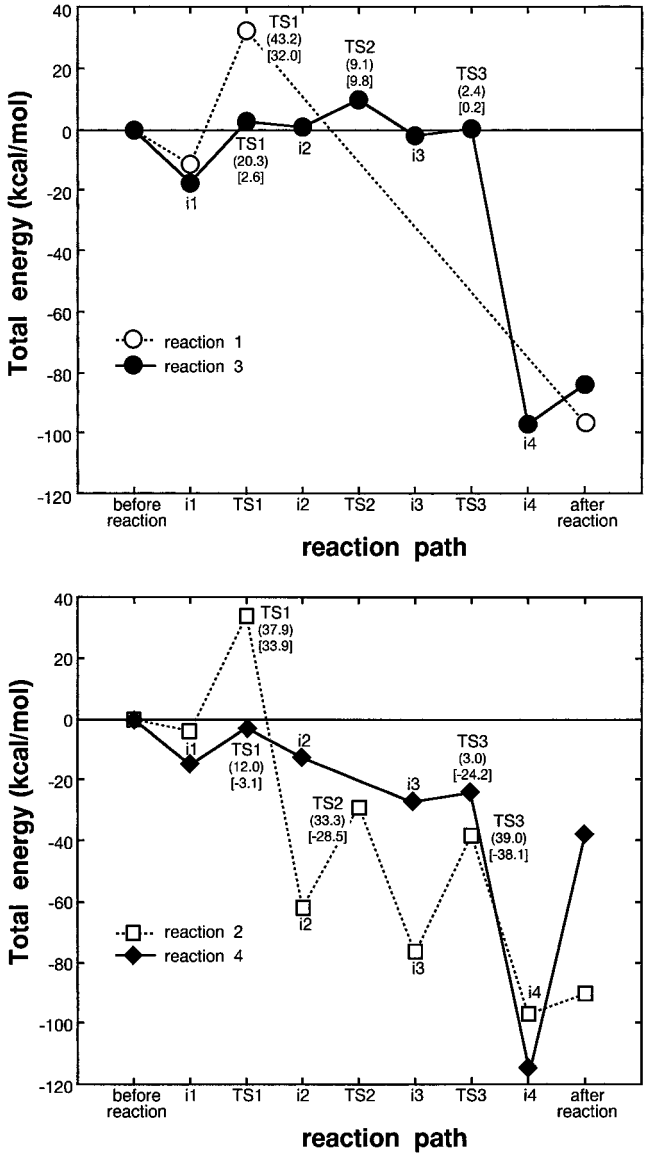

Figure 2. Energy diagrams of four reactions for the triazine ring formation of B3-LYP/6-311+G^{2d,p}//RHF/6-311G*. Values in parentheses are energy changes in kcal/mol between the preceding intermediate and TS. Values in square brackets stand for differences relative to the energy of "before reaction".

three substrate molecules participate in the ring formation equivalently. The cyanate nitrogen atom is a nucleophilic center combined with an electrophilic center, the cyanate carbon atom. Table 1 and Figure 2 show the total and relative energies, respectively, of the catalyst-free reaction. The activation energy is large, [32.0 kcal/mol] (B3-LYP/6-311+G^{2d,p}//RHF/6-311G*).Trimer association is unfavorable also due to entropy loss. In fact, the large stabilizing energy, −19.1 kcal/mol (RHF/3-21G*),[11] of intermediate **1** corresponds to the slight destabilizing energy of 1.5 kcal/mol in Gibbs free energy (Table 1). Thus, concerted ring formation without the assisting species is ruled out.

(2) Reaction with Water Molecules. Figure 3 shows the reaction including a water dimer (reaction 2). Intermediate **1** is a complex consisting of hydrogen bonds. Its deformation leads to **TS1**. At **TS1**, the reaction-coordinate vector indicates formation of C···O and N···C bonds and proton relays. The proton-relay ability of the water dimer makes the two cyanate molecules nucleophilic and electrophilic, respectively. They are then combined with a water molecule (intermediate **2**). For further progress from intermediate **2**, the imino proton needs to undergo a proton transfer (Scheme 3).

It is well-known that amino and imino protons are exchanged readily (e.g. R−NH$_2$ → R−ND$_2$ by addition of D$_2$O to an amine solution in NMR measurements). The reaction-coordinate vector indicates that the third CH$_3$-OCN molecule attacks the lone-pair orbital of the imino nitrogen atom to give a six-membered ring intermediate **3**. The intermediate undergoes a proton transfer (**TS3**) on the six-membered ring and is converted to intermediate **4**. This is composed of the product triazine ring and a water dimer. Figure 3 shows that the water assistance gives a stepwise route for the triazine formation. The facile proton relay is the driving force for yielding dimeric intermediates and six-membered ring species. Energies of reaction 2 are exhibited in Table 2 and Figure 2. The rate-determining step is **TS1** with a large activation energy ([33.9 kcal/mol] byB3-LYP/6-311+G^{2d,p}//RHF/6-311G*).[12] Thus, although reaction 2 seems to be reason-

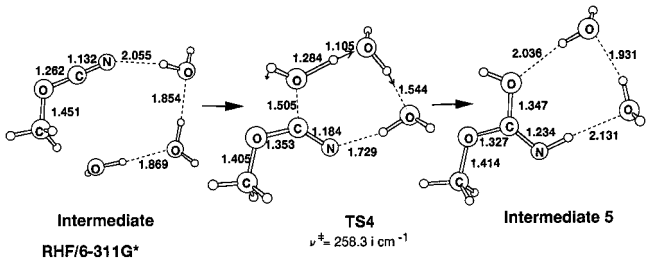

After **TS4**, an intermediate (intermediate **5**) is generated. By the following proton transfers, a more stable species, intermediate **6**, can be formed.

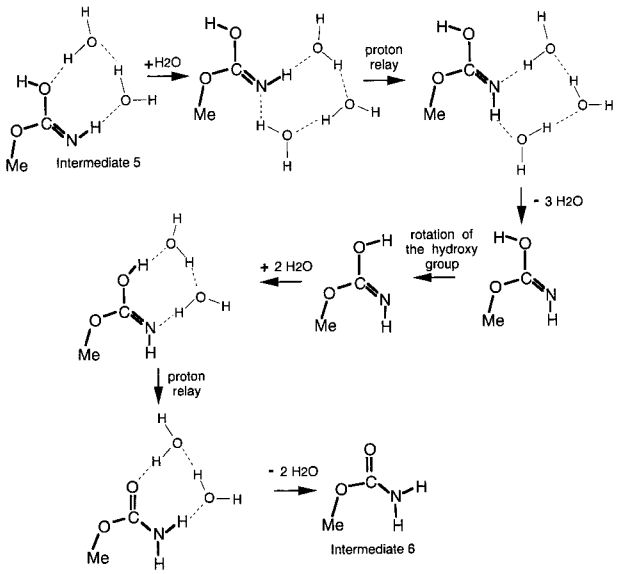

Although addition and exclusion of water molecules are arbitrarily shown above for simplicity, proton positions may be switched readily in such a way as that shown. The amide intermediate **6** was detected by ^{13}C and ^{15}N NMR spectra.[5] Thus, **TS1** and **TS4** involve the participation of four molecules and would be competitive in aqueous solution.

(11) The former stabilizing energy comes from three C−H···N hydrogen bonds. In a model methyl cyanate dimer, the hydrogen bond stabilizing energy is −6.2 kcal/mol with B3-LYP/6-311+G(2d, p)//RHF/6-311G*. The energy, 3 × (−6.2), is close to −19.1 kcal/mol of RHF/3-21G*.

(12) The cyclic form of **TS1** is composed of a water dimer and a cyanate dimer. Alternatively, the cyclic form can be made of a water trimer and a cyanate molecule. In fact, the **TS4** shown here has a geometry similar to that of **TS1**.

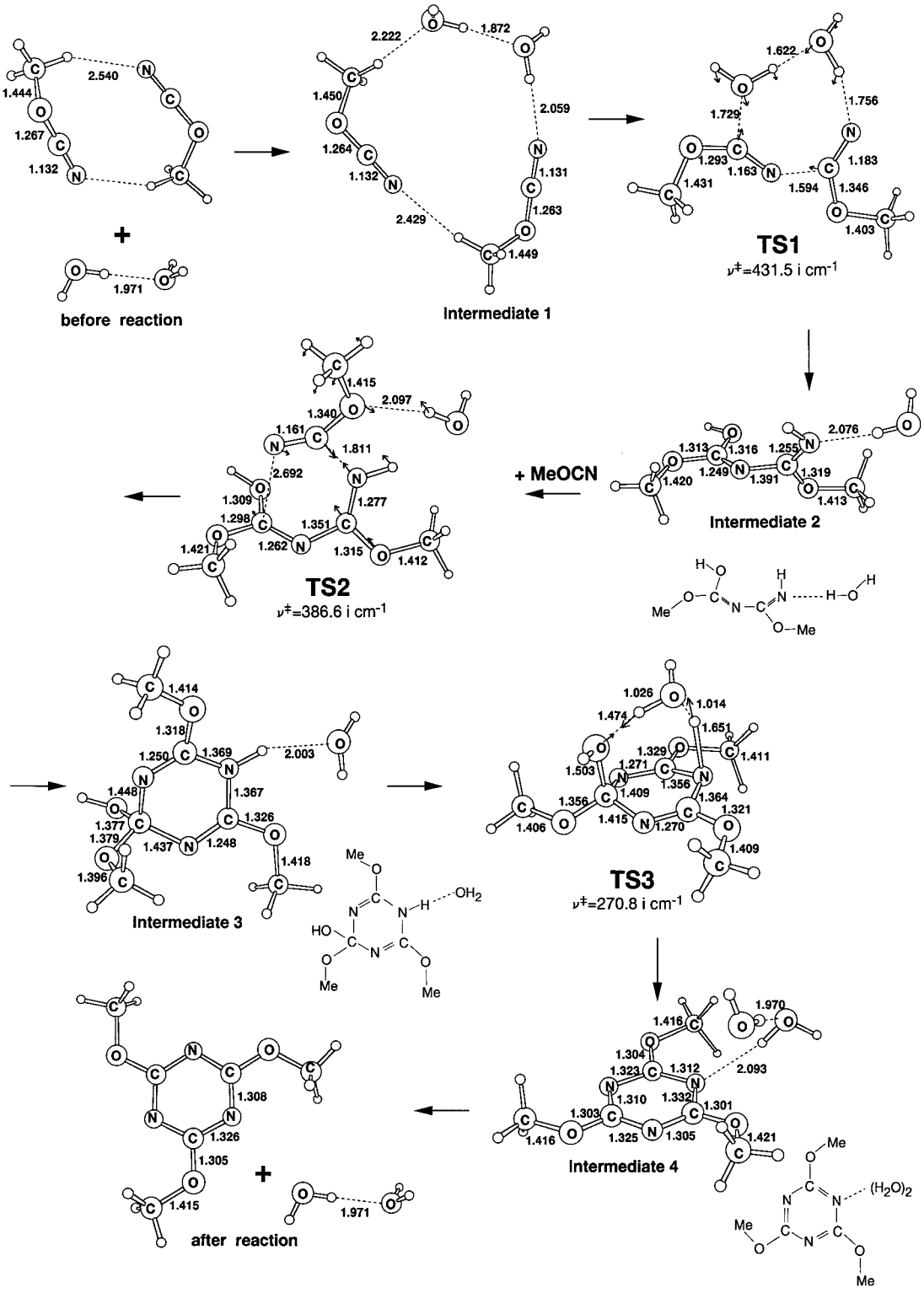

Figure 3. Geometries of the reaction assisted by water molecules. Same notations as in Figure 1 are used.

Scheme 3. Proton Transfer in Aqueous Media

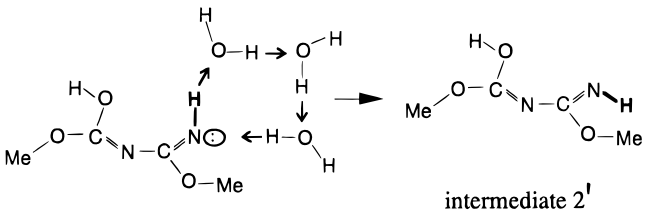

intermediate 2'

Scheme 4

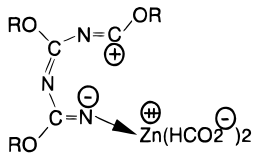

intermediate 3

Table 2. Total Energies (in hartrees) and Their Differences (in kcal/mol, parentheses) Relative to Those of $(MeOCN)_2$, $(H_2O)_2$, and MeOCN for the Water-Assisted Reaction (reaction 2). For "before reaction", "Intermediate 1", TS1, and "Intermediate 2", the Total Energy of MeOCN is Added to Those of the Optimized Geometries in Figure 3

method	before reaction	intermediate **1**	TS1	intermediate **2**	TS2	intermediate **3**	TS3	intermediate **4**	after reaction	MeOCN
RHF/3-21G	−767.993671 (0)	−768.024326 (−19.2)	−767.954344 (24.7)	−768.058667 (−40.8)	−768.044132 (−31.7)	−768.135195 (−88.8)	−768.078448 (−53.2)	−768.141691 (−92.9)	−768.114404 (−75.8)	−205.595641
free energy	−767.870823 (0)	−767.881557 (−6.7)	−767.806474 (40.4)	−767.900223 (−18.4)	−767.863877 (4.4)	−767.948363 (−48.7)	−767.956386 (−53.7)	−767.956386 (−53.7)	−767.953244 (−51.7)	−205.568106
RHF/6-311G*	−772.489937 (0)	−772.507094 (−10.8)	−772.399249 (56.9)	−772.555996 (−41.5)	−772.513808 (−15.0)	−772.604171 (−71.7)	−772.523136 (−20.8)	−772.633088 (−89.8)	−772.619686 (−81.4)	−206.801406
B3-LYP/6-311+G(2d,p)-//RHF/6-311G*	−776.962661 (0)	−776.978284 (−4.0)	−776.908684 (33.9)	−777.061173 (−61.8)	−777.008140 (−28.5)	−777.082463 (−77.1)	−777.023394 (−38.1)	−777.117021 (−96.9)	−777.106549 (−90.3)	−208.009107

Table 3. Total Energies (in hartrees) and Their Differences (in kcal/mol, parentheses) Relative to Those of MeOCN $Zn(HCO_2)_2$, MeOCN, and MeOCN ("before reaction" in Figure 4) for the Zinc-Promoted Reaction, Reaction 3

method	before reaction	intermediate **1**	TS1	intermediate **2**	TS2	intermediate **3**	TS3	intermediate **4**	after reaction
RHF/3-21G*	−2760.400296(0)	−2760.455820(−34.8)	−2760.411224(−7.5)	−2760.412717(−7.8)	−2760.382365(11.3)	−2760.409219(−5.6)	−2760.407650(−4.6)	−2760.557874(−98.9)	−2760.482265(−51.4)
FreeEnergy	−2760.281140(0)	−2760.296176(−9.4)	−2760.248133(20.7)	−2760.246721(21.6)	−2760.216935(40.3)	−2760.237061(27.7)	−2760.233086(30.2)	−2760.378174(−60.9)	−2760.325382(−27.8)
B3-LYP/6-311+G(2d,p)//-RHF/3-21G*	−2781.919645(0)	−2781.942468(−14.3)	−2781.914555(3.2)	−2781.911919(4.8)	−2781.891986(17.4)	−2781.918008(1.0)	−2781.914696(3.1)	−2781.063266(−90.1)	−2782.052437(−83.3)
RHF/6-311G*	−2774.646366(0)	−2774.678549(−20.2)	−2774.628092(11.5)	−2774.629247(10.7)	−2774.597835(30.5)	−2774.621682(15.5)	−2774.619166(17.1)	−2774.793113(−92.1)	−2774.757578(−69.8)
B3-LYP/6-311+G(2d,p)//-RHF/6-311G*	−2781.919488(0)	−2781.947616(−17.7)	−2781.915267(2.6)	−2781.918378(0.7)	−2781.903800(9.8)	−2781.922966(−2.2)	−2781.919090(0.2)	−2782.073943(−96.9)	−2782.053252(−83.9)

Table 4. Total Energies (in hartrees) and Their Differences (in kcal/mol, parentheses) Relative to Those of MeOCN, MeOCN H_3O^+, and MeOCN for Reaction 4. For "Before Reaction", "Intermediate 1", TS1, and "Intermediate 2", the Total Energy of MeOCN is Added to Those of the Optimized Geometries in Figure 5

method	before reaction	intermediate **1**	TS1	intermediate **2**	TS2	intermediate **3**	TS3	intermediate **4**	after reaction
RHF/3-21G	−692.763535 (0)	−692.790476 (−16.9)	−692.755723 (4.9)	−692.765001 (−0.9)	−692.794117 (−19.1)	−692.776039 (−7.8)	−692.931826 (−105.6)	−768.078448 (−53.2)	
FreeEnergy	−692.650611 (0)	−692.623158 (−7.3)	−692.623158 (17.2)	−692.627713 (14.4)	−692.640729 (12.5)	−692.621185 (18.4)	−692.759461 (−68.3)	−767.956386 (−53.7)	
RHF/6-311G*	−696.792931 (0)	−696.816275 (−14.6)	−696.782633 (6.5)	−696.803641 (−6.7)	−697.827962 (−22.0)	−697.807422 (−9.1)	−696.967997 (−109.9)	−772.523136 (−20.8)	
B3-LYP/6-311+G(2d,p)//-RHF/6-311G*	−700.838168 (0)	−700.862301 (−15.1)	−700.843100 (−3.1)	−700.858450 (−12.7)	−700.881612 (−27.2)	−700.876728 (−24.2)	−701.021069 (−114.8)	−777.023394 (−38.1)	

Scheme 5. The Zinc-Assisted and Stepwise Triazine Formation in Reaction 3

able structurally (Figure 3), it is unfavorable energetically. In fact, prolonged heating at 100 °C[5] and 230 °C[6] is needed for the reaction of the following substrates to occur:

The catalytic ability of water must be reconsidered in terms of higher reactivity. Thus, reaction 4 will be examined.

(3) Reaction with Zinc Formate Catalyst. Figure 4 shows geometries along the zinc-promoted reaction (reaction 3). In the geometry entitled "before reaction", the zinc atom is bound to the cyano nitrogen atom. This coordination enhances the electrophility of the cyano carbon atom. Intermediate **1** is a reactant-like complex which involves, however, only weak intermolecular attractions. The electrophility does not effect the formation of any covalent bonds of intermediate **1**. After intermediate **1**, **TS1** has been obtained. In **TS1**, a C···N bond is formed, as the reaction-coordinate vector shows. The resultant stable species is intermediate 2. The N−Zn distance is 1.933 Å which is shorter than 2.132 Å in the"before reaction". The shortening indicates that the cyanate dimer is a stronger electron donor than the monomer. After intermediate 2, the second C···N bond is formed in **TS2** according to the vector movement. **TS2** is followed by formation of intermediate 3. Noteworthy is the geometry of intermediate 3,which is ready for the last C···N bond formation to give the triazine ring (Scheme 4). This is **TS3** where the vector indicates the formation, and intermediate 4 is formed. Intermediate **4** is the product, triazine, coordinated by the zinc catalyst.

It can be reasonably explained that the zinc catalyst has brought about the stepwise C···N bond formation. In fact, activation energies of **TS1**, **TS2**, and **TS3** are small (2.6, 9.8, and 0.2 kcal/mol by B3-LYP/6-311+$G^{2d,p}$//RHF/6-311G*) in Table 3 and Figure 2. **TS2** is the rate-determining step, which comes from the slight difficulty of forming the second C−N bond. Thus, a small amount of zinc catalyst greatly enhances triazine formation. The driving force is a large polarization of the cyano group by the catalyst.

(4) Reaction with the Hydronium Ion Catalyst. Reaction 2 (Figure 3) is a stepwise process assisted by water molecules, but it requires a relatively large activation energy. Reaction 3 involves a stepwise path and is favorable on account of the effective zinc catalysis. The role of the aqueous media on the triazine formation is reconsidered here. The catalyst is modeled by a hydronium ion (H_3O^+). In the case of ion, the catalytic strength

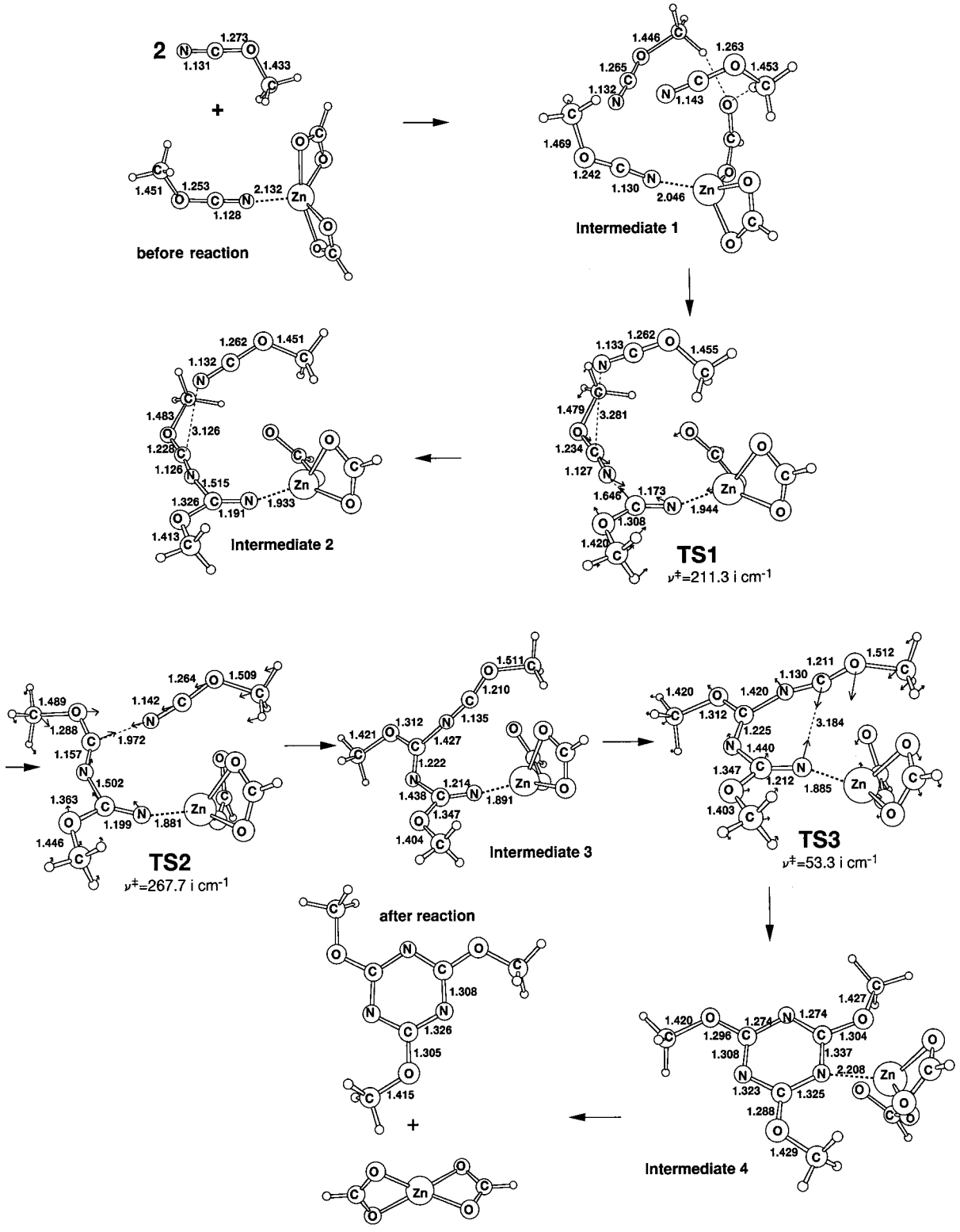

Figure 4. Geometries of the reaction catalyzed by zinc formate. The binding energy for the complex of methyl cyanate with zinc formate is 12.5 kcal/mol with B3-LYP/6-311+G^{2d,p}//RHF/6-311G*.

is too strong to simulate the reaction in the aqueous media, and actually $H_3O^+(H_2O)_n$ (n: large)clusters may reproduce the proper catalytic strength. But calculations including a $H_3O^+(H_2O)_n$ cluster are difficult. The position of water molecules is varied in many ways during geometry optimizations. Consequently, the hydronium ion is adopted here as a catalyst. Figure 5 shows geometric changes in reaction 4 (total energies are shown in Table 4). A stepwise path has been obtained, which is similar to that of the zinc catalyst (Figure 4).

Concluding Remarks

This study has dealt theoretically with the fundamental mechanism of the cyanate-resin formation. The trimeric triazine ring cannot be made concertedly. Reaction

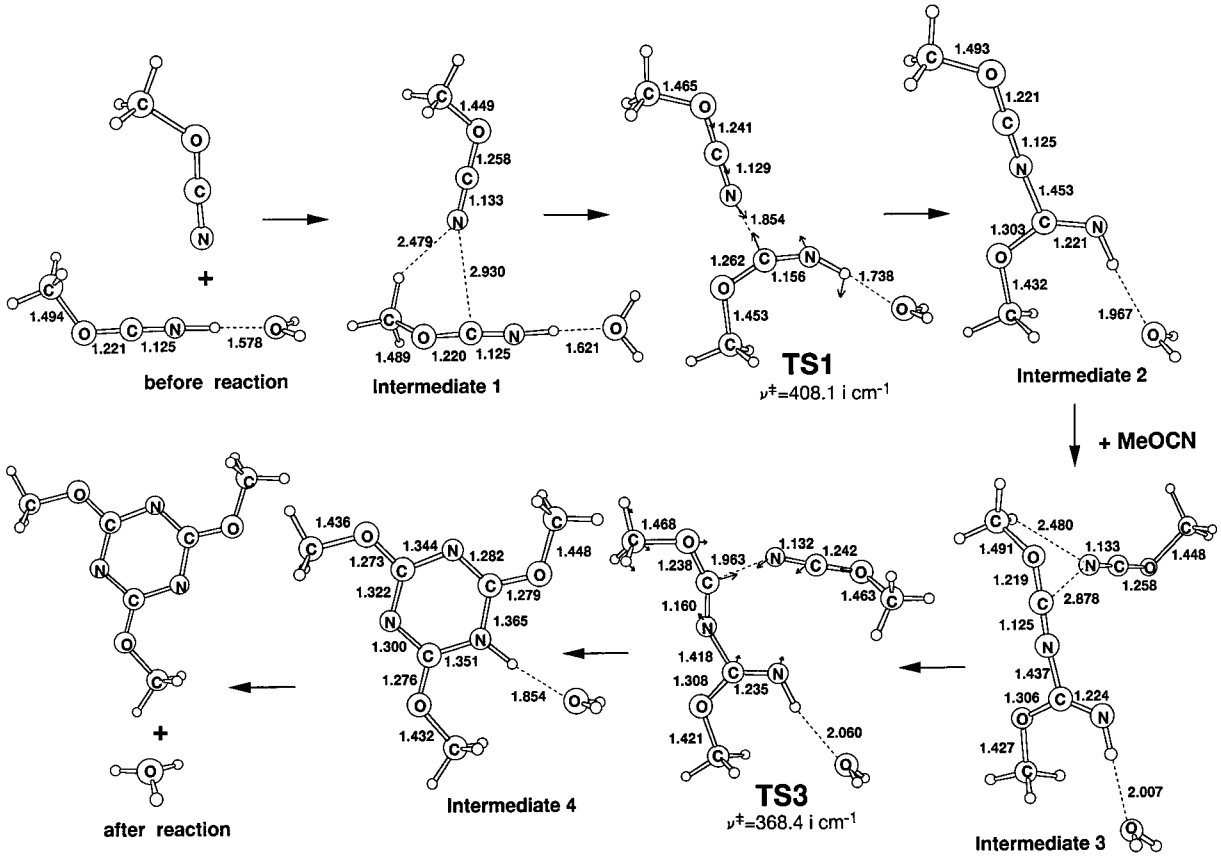

Figure 5. Geometries of the reaction catalyzed by hydronium ion.

1 is unfavorable both energetically and entropically (Figure 1). When water is added to the cyanate solution, the complete neutral condition gives a stepwise route (Figure 3). Although smooth proton relays are involved in reaction 2, the first addition (TS) is of large activation energy. The neural water clusters do not necessarily have enough catalytic strength to cause facile successive C−N formations. The zinc catalyst brings about a reasonable route (Figure 4 and Scheme 5) in reaction 3.

Industrially, zinc octanoate is often used instead of the zinc formate. However, judging from the geometries of Figure 4, this kind of carboxylate is insensitive to the reaction route. Two C−H bonds of formate ions are far from the reaction center. The reaction would be accelerated by a small amount of stronger Lewis acids such as BF_3. The hydronium ion may give a similar stepwise path (reaction 4). At this path, attachment of the third cyanate and ring closure take place at the same time. A weak acid condition would enhance the curing reaction.

Supporting Information Available: Cartesian coordinates of geometries optimized with RHF/6-311G*of all species in Figures 1, 3, 4, and 5. This material is available free of charge via the Internet at http://pubs.acs.org.

JO9900275